R. Wei[1]

B. Shogrin

P. J. Wilbur

Department of Mechanical Engineering,
Colorado State University,
Fort Collins, CO 80523

O. Ozturk

D. L. Williamson

Department of Physics,
Colorado School of Mines,
Golden, CO 80401

I. Ivanov
Charles Evans & Assoc.
Redwood City, CA 94063

E. Metin
Department of Materials and
Metallurgical Engineering,
New Mexico Institute of
Mining and Technology,
Socorro, NM 87801

The Effects of Low-Energy-Nitrogen-Ion Implantation on the Tribological and Microstructural Characteristics of AISI 304 Stainless Steel

The effects of nitrogen implantation conditions (ion energy, dose rate, and processing time) on the thickness and wear behavior of N-rich layers produced on 304 stainless-steel surfaces are examined. Surfaces implanted at elevated temperatures ($\approx 400°C$) with 0.4 to 2 keV nitrogen ions at high dose rates (1.5 to 3.8 mA/cm^2) are compared to surfaces implanted at higher energies (30 to 60 keV) and lower current densities (0.1 to 0.25 mA/cm^2). The most wear-resistant surfaces are observed when the implanted-ion energy is near 1 keV and the dose is very large ($>2\times10^{19}$ ions/cm^2). Typically, surfaces implanted under these optimum conditions exhibit load-bearing capabilities at least 1000 times that of the untreated material. Some comparisons are also made to surfaces processed using conventional plasma-nitriding. Samples treated using either process have wear-resistant surface layers in which the nitrogen is in solid solution in the fcc phase. It is argued that the deep N migration ($>1\mu m$) that occurs under low-energy implantation conditions is due to thermal diffusion that is enhanced by a mechanism other than radiation-induced vacancy production.

Introduction

Nitrogen-ion implantation (Bolster and Singer, 1980; Yost et al., 1983; Singer et al., 1988) and plasma nitriding (Szasz et al., 1989; Edenhofer, 1974) are both processes that involve the delivery of energetic ions into materials and yield nitrogen-rich surface-layers that resist wear. Plasma nitriding is, however, much more widely employed commercially than implantation, possibly because 1) it utilizes nitrogen ions with much lower energies, 2) it has typically been accomplished at higher temperatures so that thicker layers are produced, and 3) it always involves immersion and therefore, relatively uniform coverage of geometrically complex component-surfaces. Recently, however, studies of elevated-temperature, nitrogen-ion implantation (Wei et al., 1991a; Williamson et al., 1991) have shown that this process can be controlled in such a way that rapid diffusion similar to that observed in plasma nitriding occurs. In addition, component-immersion, nitrogen-ion implantation yielding uniform coverage has been demonstrated using techniques designated as plasma-source ion implantation (Conrad et al., 1987; Shamim et al., 1991) and plasma-immersion ion implantation (Tendys et al., 1988; Hutchins et al., 1992). Thus, the only significant differences between the two processes appear to be the energy and flux (or current density) at which ions are delivered into the treated surface. The principal objective of this paper is to examine the effects of changing the energy and flux under controlled conditions and to seek the common ground between the two processes that could facilitate definition of optimum processing conditions for both techniques. The bulk of the work has been conducted using samples prepared in implantation facilities that afford precise process control. However, two samples were plasma-nitrided under conditions that facilitate direct comparison with layers produced using nitrogen implantation.

Over the past two decades, nitrogen-ion implantation has been shown to improve the tribological properties of austenitic stainless steels (Bolster and Singer, 1980; Yost et al., 1993). The authors have further demonstrated (Wei et al., 1991a and 1991b) that high-dose implantation ($>4\times10^{17}$ N_2/cm^2) at an energy of 60 keV increases the load-bearing capacity of AISI 304 stainless steel (SS) by two to three orders of magnitude,

[1]Present address: Hughes Research Laboratories, Malibu, CA.

Contributed by the Tribology Division for publication in the JOURNAL OF TRIBOLOGY. Manuscript received by the Tribology Division March 11, 1993; revised manuscript received March 24, 1994. Associate Technical Editor: K. Komvopoulos.

provided the material is held at a temperature near 400°C during implantation. Microstructural studies by the authors (Williamson et al., 1991) have also shown that increases in dose and temperature lead to the sequential formation of different nitrogen-containing phases [ε-(Fe, Cr, Ni)$_x$N, N in solid solution and CrN] and progressive increases in wear resistance with these sequential changes. Under these processing conditions nitrogen diffuses at a rate that yields nitrogen-bearing layers that are over 10 μm thick in about an hour. However, since the formation of CrN accompanies the degradation of the corrosion resistance of 304 SS (Zhang and Bell, 1985; Chabica et al., 1992), it will generally be desirable to avoid implantation at the higher temperatures (>450°C) where Cr becomes sufficiently mobile to precipitate as CrN. Implantation at a more moderate temperature (≈400°C) and doses ranging to 1×10^{18} N_2/cm^2, however, induces the formation of nitrogen in solid solution and this phase shows a preferred combination of both wear and corrosion resistances.

The mechanism through which nitrogen implanted at an elevated temperature migrates hundreds of times the ballistic implantation range (Ziegler et al., 1985) has been the subject of considerable research. A highly regarded theory (Rehn et al., 1985) holds that bombardment by the energetic ions results in the formation of near-surface vacancies and their movement enhances the normal thermal-diffusion mechanism (Strack, 1963; Jones and Martin, 1964; Hudis, 1973). This theory does not seem to be supported, however, by experiments in which thicker layers were produced at low ion energies where vacancy yields should be lower. These low-energy experiments have involved both plasma-nitriding (Zhang and Bell, 1985) and ion-implantation techniques (Byeli, 1992). A recent paper by the authors (Williamson et al., 1994) in fact, shows that published thermal-diffusion coefficients are generally inadequate to explain measured layer thicknesses and a model that does not invoke radiation-enhancement effects is proposed. In any event, the similarity of plasma-nitriding and low-energy ion-implantation processes suggests that the nitrogen-diffusion mechanism should be similar for both.

Procedures and Apparatus

Test Sample Preparation. Commercial-quality AISI 304 stainless steel was selected for this study because it is a widely used engineering material with surface properties which can be enhanced by the introduction of nitrogen. Wear-test disks 5 cm in diameter were machined from AISI 304 sheet and polished on one surface to a mean roughness $R_a=0.01$ μm. After sequential ultrasonic cleaning with chlorothene, acetone, and methyl alcohol, they were either wear tested, to obtain baseline (untreated disk) data, or placed in a vacuum chamber for implantation or nitriding.

Ion Implantation and Nitriding. In order to separate the effects of nitrogen-ion energy, current density, and thermal diffusion on the tribological and microstructural characteristics of the disks, and to facilitate meaningful comparisons with plasma-nitriding results, the times of, and disk temperatures during ion implantation were held constant while ion energy and current density were varied. As illustrated in a previous paper (Wei et al., 1991b), gross temperature control of each disk was achieved by clamping a 0.38 mm thick sheet of flexible graphite ("grafoil") and various numbers of mica sheets (~0.06 mm thick) on the side of the disk opposite the ion beam between the disk and a water-cooled heat sink on which the disks were mounted. Temperature was sensed using a copper-constantan thermocouple clamped between the disk and the relatively soft grafoil. Secure clamping of each disk against the grafoil at both its center and around its periphery assured temperature uniformity over the disk surface.

The means of achieving fine temperature control is illustrated in Fig. 1, which shows current-density and temperature histories for a typical disk. As Fig. 1 suggests, the implantation process begins at a high current density that is sustained for the short time required to heat the disk to the prescribed processing temperature. The current density is then reduced and varied about the level required to maintain that temperature. One-dimensional heat-transfer analysis shows the temperature on the beam side of the disk is only about 20°C greater than that sensed by the thermocouple under the highest input-power conditions. An implantation temperature of 400°C was selected for most of the disks used in this study because previous work (Williamson et al., 1990) had shown that high-energy nitrogen implantation (60 keV) at this temperature resulted in the formation of a high-strength, nitrogen-in-solid-solution phase. The processing time indicated in Fig. 1 is the interval between the times when the prescribed temperature (400°C) is first reached and implantation is stopped. This time interval at 400°C is the appropriate one because the N diffusion rate decreases dramatically as temperature is reduced. Two processing times (10 and 30 min) were used to enable comparison with previous results. In order to continue to meet the 400°C implantation-temperature specification as implantation energy is reduced, the current density was increased to maintain power density relatively constant.

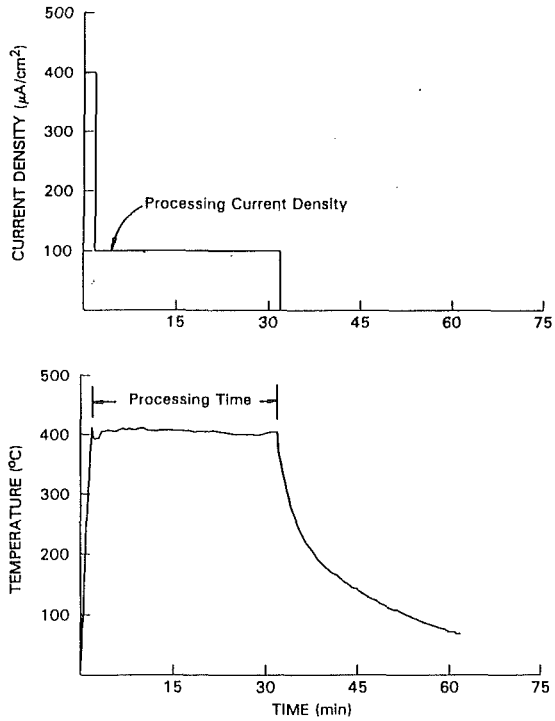

Fig. 1 Typical implantation-current-density/disk temperature history

Two broad-beam ion implanters were used for this work, one for high implantation energies (30–60 keV) (Wilbur and Daniels, 1986) and the other for low energies (0.4–2 keV). Strictly speaking, the low-ion-energy system would probably not be classified as an implanter because the associated energies are sufficient to deliver ions no more than a few atom-layers below the surface. When the disks are maintained at an elevated temperature, however, the resulting neutralized atoms can diffuse inward, thereby producing thick, nitrogen-rich layers.

The processing conditions for each disk investigated (ion energy, beam current density, total dose, and processing time) are listed in Table 1. It shows that most disks were implanted at 400°C for either 10 or 30 min but one disk was implanted at 400°C for 125 min and two others were implanted for 10 and 30 min at a higher temperature (475°C). These three samples were designed to simulate conventional nitriding, which

Table 1 N-implantation/nitriding comparisons for 304 SS discs

Implantation/nitriding						
Ion energy (keV)	Dose rate (mA/cm^2)	Dose (N_2/cm^2)	Time/temp. (min/°C)	Predominant Nitride[a]	Layer Thickness[b] (μm)	Critical load (N)
60	0.1	1.0×10^{18}	30/400	γ_N(p)	1.0*	51
30	0.25	3.5×10^{18}	30/400	γ_N(m)	1.0*	61
2	1.5	2.3×10^{19}	30/400	γ_N(m)	2.0*	>100[c]
1	2.2	3.5×10^{19}	30/400	γ_N(m)	3.1	>100[c]
0.7[d]	2.5	4.7×10^{19}	30/400	γ_N(m)	2.6	93
0.7[d]	2.5	4.8×10^{19}	30/400	γ_N(m)	2.0*	40
0.4	3.75	6.3×10^{19}	30/400	γ_N(m)	1.9	35
0.4[e]	—	—	30/400	γ_N(m)/γ_N(p)	1.0*	8
60	0.13	9.0×10^{17}	10/400	γ_N(p)	1.6	76
30	0.25	1.8×10^{18}	10/400	γ_N(p)	1.5	72
2	1.5	9.0×10^{18}	10/400	γ_N(m)	1.9	90
1	2.2	1.6×10^{19}	10/400	γ_N(m)	2.4	>100[c]
0.7[d]	2.5	2.4×10^{19}	10/400	γ_N(m)	2.3	>100[c]
0.7[d]	2.5	2.6×10^{19}	10/400	γ_N(m)	1.7	>100[c]
0.4	3.75	3.8×10^{19}	10/400	γ_N(m)	1.4	23
0.4[e]	—	—	10/400	γ_N(p)	0.7	15
1	3.4	4.8×10^{19}	30/475	CrN	6.5	>100[c]
1	2.5	1.7×10^{19}	10/475	(f)	2.3	>100[c]
1	2.0	1.0×10^{20}	125/400	γ_N(m)	4.5	>100[c]

[a] Determined from CEMS, CXMS and XRD.
[b] Layer thicknesses determined by XRD and CXMS with confirmation by AES in cases with *.
[c] Critical Loads for these disks exceeded the load capacity of the tribotester (100 N).
[d] Two disks were implanted to study reproducibility.
[e] Designates layer produced by plasma nitriding-current densities and therefore doses are not known for these disks but other processing parameter are given in the text.
(f) Complex mixture of nitrides.

is done for longer times to generate much thicker layers (≈0.1 mm) and is usually carried out at higher temperatures (>500°C) to promote more rapid diffusion. The disks that were plasma nitrided were treated using a commercial process (Inal and Robino, 1982). They were maintained at 400°C for 10 and 30 min so the results obtained could be compared directly to results from the nitrogen-implantation tests. Nitriding was accomplished by first biasing the disks 300 V negative with respect to ground in a vacuum chamber that contained hydrogen at a pressure of 9 Torr. Under these conditions a glow discharge is established, and positive hydrogen ions produced in this discharge are drawn toward the disk. These ions, which have energies that range to the applied voltage, condition and clean the disk. Next, the disk was nitrided by changing the gas to a mixture of 15 vol. percent N_2 and 85 vol. percent H_2 at a pressure of 9 Torr and adjusting the voltage to 400 V.

Wear Testing. All disks were subjected to sliding wear testing using an oscillating pin-on-disk tribometer (Wei et al., 1990) that produces a broad wear band (~1 cm wide) on the disk. The tribometer was operated at a mean sliding speed of 13 cm/s while a boundary lubricant (10 vol. percent oleic acid in kerosene) was flushed onto the disk near the pin/disk contact region to lubricate the contact and remove wear debris. The counter-surfaces for the tests were hard WC pins (4000 kg/mm^2 Vickers) which had a 3.2 mm-radius of curvature and had been polished to a mean roughness $R_a=0.2$ μm. On the basis of a previous study (Wei et al., 1991b), which showed that implanted nitrogen increases the load at which 304 SS undergoes the transition from mild-to-severe adhesive wear, the critical load associated with this transition was measured to establish the tribological performance of each disk. This was accomplished by first applying a low normal load (0.1 N) and subjecting the disk to sliding wear for a period of one hour. The wear-rate of a disk was determined by removing it after each 1-h interval, weighing it using a balance accurate to within ±11 μg, and converting the weight loss to a volume loss using the density of 304 SS. If the measured wear rate was low (typically $<10^{-7}$ mm^3/N/m) the normal load was increased to 1 N, and the 1-h wear test and weighing sequence was repeated. Incrementing the load, wear testing the disk, and measuring its wear rate continued until the treated layer either failed and the wear rate rose dramatically and suddenly (into the range 10^{-4} mm^3/N/m), or the load capacity of the tester (100 N) was reached. At this test-machine limit, the Hertzian contact stress of 4.4 GPa (computed by assuming that the implanted layer has the same Young's modulus and Poisson's ratio as the substrate) was much greater than the yield strength of 304 SS (0.21 GPa). Additional detail on this testing procedure is given elsewhere (Wei et al., 1990, 1991a and 1991b).

Implanted-Layer Analyses. Conversion electron Mössbauer spectroscopy (CEMS), conversion X-ray Mössbauer spectroscopy (CXMS) and X-ray diffraction (XRD) were used to study the nitrides that had formed during implantation and any nitride transformations that may have occurred during wear testing. Sometimes a small sample was cut from the region of an implanted disk that was not worn and Auger electron spectroscopic (AES) examination was performed so implanted nitrogen and contaminant profiles could be measured. No significant contamination (C or O) was found in any treated layers.

Ultra-light-load-microhardness (Vickers) measurements were also made on selected samples. The lowest normal load that could be applied with the equipment used to make these measurements was 0.005 N. Indentations in treated surfaces produced by loads extending from this level up to 0.05 N had small diagonals (≈0.5 to 2 μm) that were measured using a scanning-electron microscope. This diagonal range corresponded to a depth range of ≈0.1 to 0.4 μm.

Results

As-Implanted, Near-Surface Concentrations and Microstructures. Figure 2 shows nitrogen-concentration depth profiles measured by AES on implanted and nitrided 304 SS disks that were each processed for 30 min at different ion-energy and current-density conditions. Except for the nitrided disks, where it was not measured, the current density required to induce a 400°C disk temperature is shown parenthetically beneath each implantation energy. For comparison, a ballistic

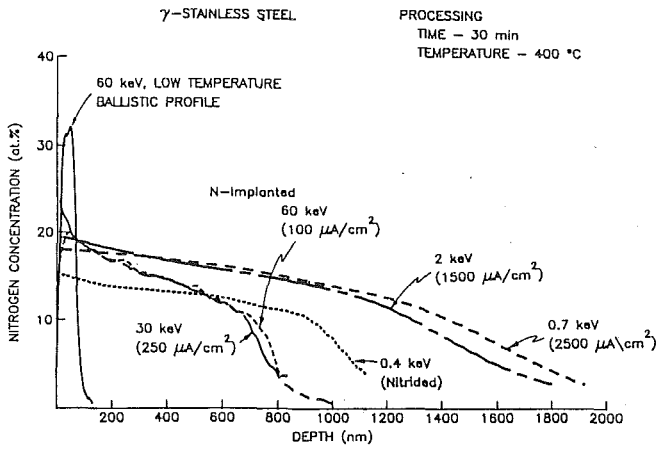

Fig. 2 Representative Auger-electron-spectroscopic (AES) N-concentration profiles (the absolute N concentrations may be inaccurate because AES sensitivity factors are not known for the high-N phase in 304 SS)

profile measured when this material is implanted under low-temperature, high-energy conditions (<300°C, 60 keV, respectively) is also shown. Comparison of the profiles clearly shows that the elevated-temperature implantation and nitriding processes both yield N-rich layers that are at least an order of magnitude thicker than the ballistic depth. It is also apparent 1) that implantation at 0.7 to 2 keV at the high current densities (1.5–2.5 mA/cm^2) yields the thickest layers and 2) that implantation yields higher N concentrations than nitriding. In addition the N concentrations in all the disks processed at 400°C can be seen to be close to the Cr atom concentration in the 304 SS alloy (nominally 19 at. percent) and XRD analyses suggest the N concentration in the solid solution is even higher than that indicated in the AES data of Fig. 2. These results are consistent with a qualitative model proposed by Williamson et al. (1992 and 1994). The model suggests 1) that N solubility is effectively enhanced by N trapping near Cr atoms, which are relatively immobile at 400°C and 2) that N added to a saturated region via implantation migrates more readily than it would in low-nitrogen SS. The thicker layers shown in Fig. 2 for the lower energy implantation cases suggest that diffusion rates are enhanced as these energies are reduced and current densities are increased.

After nitrogen introduction and before wear testing, each disk was also examined using CEMS, CXMS, and XRD to determine the nitride phase(s) formed. The dominant near-surface nitride phases and layer thicknesses determined by analysis of these data are summarized in Table 1. This table shows the disks retained substantial nitrogen in solid solution as magnetic $\{\gamma_N(m)\}$ and/or nonmagnetic or paramagnetic $\{\gamma_N(p)\}$ phases in the near-surface layer. X-ray diffraction analyses confirm these phases and show evidences of high internal stresses associated with the $\gamma_N(m)$ phase (≈2 GPa) (Williamson et al., 1994). The data in the table generally suggest the thickness of the $\gamma_N(m)$ and/or $\gamma_N(p)$ phases reaches a maximum near the 1 keV/2.5 mA/cm^2 condition. Note for the higher energy implants (60 and 30 keV) the 10-min processing time apparently yields thicker layers than the 30-min one while for the lower energy implants the layer thicknesses are greater for the 30-min time. However, the latter are not the factor of $\sqrt{3}$ thicker that would be expected if simple diffusion were controlling. Either a high sensitivity to temperature or unusual effects in the initial stages of the process seem to be playing a role.

When a disk was implanted for a longer time (125 min versus 10 or 30 min), the same solid-solution phases were formed {predominantly $\gamma_N(m)$} and the N-rich layer was about twice as thick as those implanted for short times. This thickness is

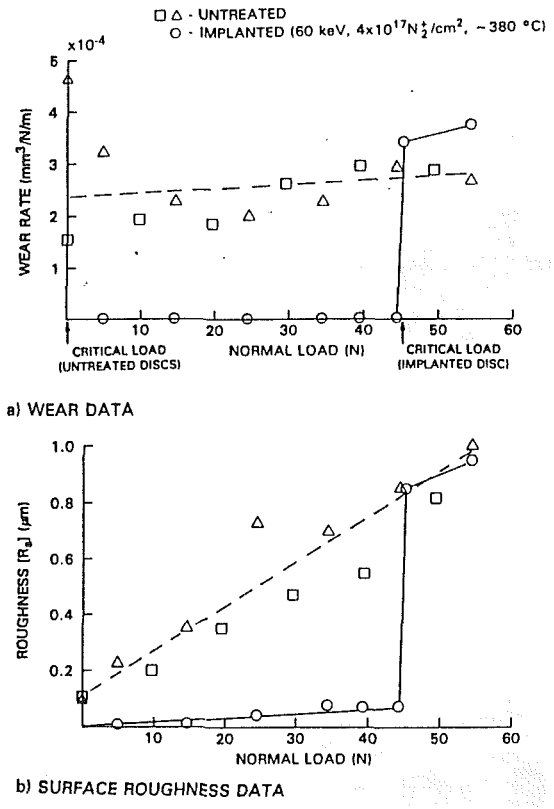

Fig. 3 Typical critical-load measurements made on 304 stainless steel disks using an oscillating-pin-on-disk tribometer (lubricated sliding at 13 cm/s)

reasonably consistent with the assumption of a diffusion-controlled process (i.e., $\sqrt{125/30} \approx 2$). When disks were implanted at 475 rather than 400°C, CrN precipitates in a bcc FeNi-matrix, rather than a solid-solution phase, was formed. This result is similar to one obtained when N was implanted at 500°C and 60 keV (Wei et al., 1991a and Williamson et al., 1991). Finally, it is observed that 1) nitriding yields layers that are thinner than those produced by N implantation at the same energy and time and 2) the nitrided layer thickness determined by AES (Fig. 2) is consistent with that determined by XRD and CXMS (Table 1).

Wear Testing. After nitrogen treatment and the completion of CEMS, CXMS, and XRD measurements, the disks were subjected to wear testing. Typical results comparing disk wear-rates and roughnesses (R_a) for untreated and implanted disks as normal load was increased incrementally are shown in Fig. 3(*a*). One can see high and relatively uniform wear-rates for the untreated disks are realized over the full range of normal loads applied (0.1 to 55 N). On the other hand, the implanted disk shows wear below the mass-loss-measurement limit after a 1 h test (i.e., $<10^{-7}$ mm^3/N/m) up to a normal load of 45 N. The appearance of a typical region in the broad wear band on the disk surface after 1 h of testing at this load is shown in Fig. 4(*a*). This surface shows evidence of mild plastic deformation, including some surface tearing normal to the score lines that lie in the direction of pin travel but the surface is still essentially intact. Although a mild adhesive wear mechanism appeared to prevail up to this 45 N normal load, within a few minutes after the normal load had been increased to 46 N the surface appearance changed dramatically. The wear rate and roughness after 1 h of testing at this load were at values typical of an untreated disk (Fig. 3) and the appearance was also the same as that for an untreated disk (Fig. 4(*b*)). These changes, which are typical, all indicate the im-

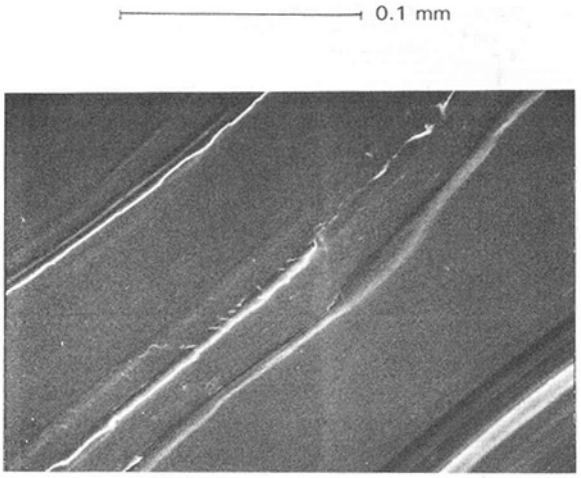

a) BELOW CRITICAL LOAD (45 N)

b) AT CRITICAL LOAD (46 N)

Fig. 4 Scanning electron micrographs of nitrogen-implanted disk surfaces (60 keV, 4 × 10^{17} N_2^+/cm^2, ~380°C) near critical load

planted layer fails and is removed from the surface by the pin at the critical load (46 N in the example). The disk then experiences severe adhesive wear (galling) of the untreated material beneath the layer. For the untreated disks, the critical load was less than the lightest load that could be applied (0.1 N). As the data of Fig. 3(*b*) suggest, the roughnesses of the untreated disks increased with load until, at a 45 N load, their surfaces looked the same as the one shown in Fig. 4(*b*).

The critical loads measured for each of the disks tested in this study are listed in the last column of Table 1. All of these loads are dramatically greater than the critical load of untreated 304 SS (at least 80 to 1000 times greater). The effect of ion energy and current density on critical load given by these data for both 10- and 30-min treatment times are summarized in Fig. 5. It shows that the critical load, which is small for disks treated using 0.4 keV energy ions at the highest current density (3.75 mA/cm^2), increases rapidly to values beyond the load limit of the test apparatus (100 N) for ion energies near 1 keV and then decreases at higher energies and lower current densities. Both the 10 and 30 min processing-time data fall within or are close to the shaded band on the figure, suggesting that these processing-time variations induce changes within the range of experimental error.

The results of Fig. 5 and Table 1 show that the disks implanted and nitrided at 0.4 keV all have thinner layers and lower critical loads than those implanted at 1 and 0.7 keV even though current densities were greater for the disks implanted at 0.4 keV. This suggests that much of the nitrogen that impacts on the disk surfaces at this low energy is not diffusing inward. It is considered noteworthy that the three disks implanted for either a longer time (125 min) or at a higher temperature (475°C), had critical loads that exceeded the load capability of the tester (> 100 N). These high critical loads correlate with the thicker N-containing layers that were measured. In fact, generally the results of Table 1 show that thicker layers yield higher critical loads. The high critical load observed in the 475°C/30 min disk is also consistent with the fact that CrN formed in an α-FeNi matrix and this phase has been shown to have a higher critical load than N in solid solution (Wei et al., 1991a).

Microstructural analyses were also performed periodically during the wear testing of some disks to determine the extent to which nitride phase transformations were induced by the wear testing itself. These measurements showed that nitrogen phases formed during implantation/nitriding do not transform as a result of wear testing. However, transformation of the substrate to martensite was observed by CXMS and XRD for tests that had been conducted at those high normal loads where the machine limit was reached before the critical load. These results suggest 1) that high normal loads cause the softer substrate material near an interface with a harder N-rich layer to deform plastically and 2) that this leads to the initiation of failure at the interface. This mode of failure and the trend for critical load to increase with layer thickness that is shown in the data of Table 1 are both consistent with predictions of Komvopoulos (1989). Once failure initiates at the interface, physical observation suggests the layer flakes off rapidly and severe wear of the substrate material follows.

Microhardness Measurements. Typical Vickers microhardness (H_v) data for selected disks measured as a function of indenter load are given in Fig. 6. They show a general trend for the hardness to increase as the indenter load is reduced. This occurs because the measurement is influenced primarily by the substrate at heavy loads where indenter penetrates deeply and primarily by the layer at light loads where indenter penetration is shallow. The data in Fig. 6 show this effect for all of the disks implanted at 400°C and for the nitrided disk (also at 400°C), which has the lowest hardness value. Actually, disks implanted at energies ranging from 0.4 to 60 keV and a temperature of 400°C had hardness that fell within a narrow range (represented by the bars through the square data symbols in Fig. 6). The disk implanted for the longest time (125 min) exhibits hardness values that are quite insensitive to indenter load, and this is consistent with the thicker N-rich layer observed in this case (see Table 1).

When the disk was implanted at 475°C, the CrN phase formed, and Fig. 6 shows the hardness values were then higher at greater indenter loads. The high hardness at the heaviest load (0.5 N) confirms the datum of Table 1 which shows a thicker layer. These data also suggest the hardness of the CrN in α-FeNi microstructure may be greater than that of pure CrN [1083 kgf/mm^2] (Peterson and Ramalingam, 1981). The fact that layer thickness increased significantly when implantation temperature was increased from 400 to 475°C provides strong evidence that thermal effects have a dominant influence on low-energy-implantation/nitriding processes.

The hardness of untreated 304 SS is not included explicitly in the data of Fig. 6, but it is suggested by the values at high loads for the samples processed for 30 min (250–350 kgf/mm^2). This range is consistent with other measurements made on untreated 304 SS made over the full load range of Fig. 6 (Wei et al., 1991b).

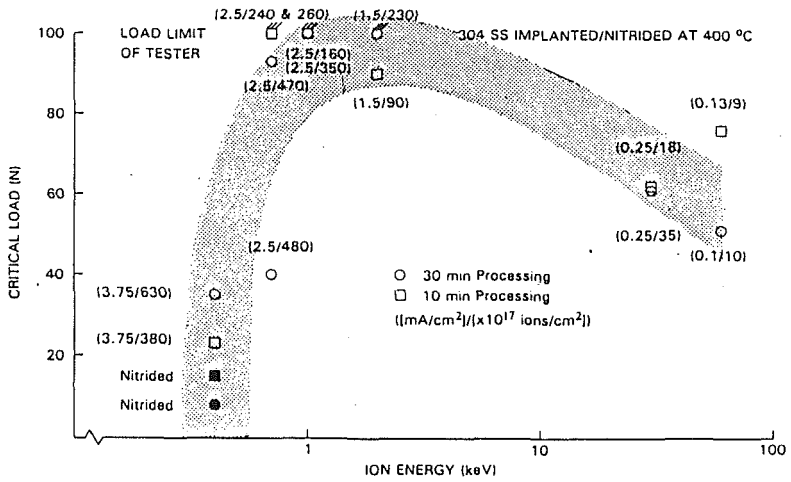

Fig. 5 The effect of implantation energy and (current density/dose) on critical load

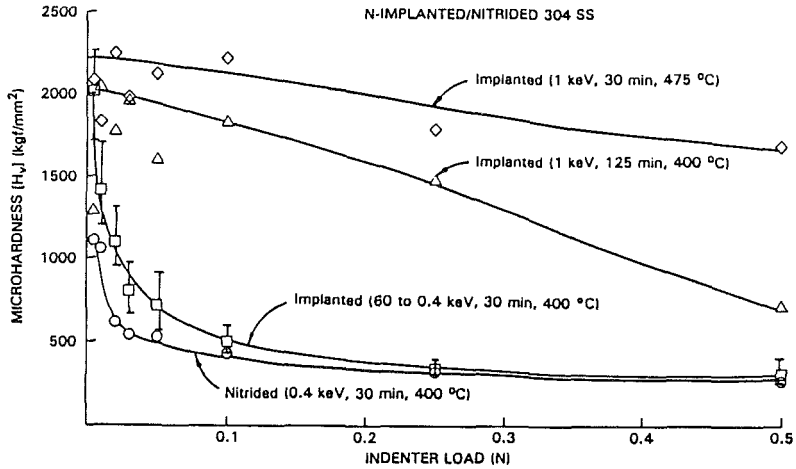

Fig. 6 Representative microhardness results (square symbols and vertical bars indicate mean values and ranges, respectively)

Discussion

Taken together, the preceding results show that elevated-temperature, low-energy nitrogen implantation of 304 SS at high current densities to high doses produces thick surface-layers in which N concentrations are near a saturation limit which may be as great as 40 at. percent (Williamson et al., 1994). A metastable, high-N solid solution phase is generally produced in these layers and it improves the load-bearing capacity of the material dramatically. The constraint of N delivery at a prescribed temperature that has been imposed in these tests corresponds to delivery at similar power densities, so increases in ion energy must be accompanied by corresponding reductions in ion current density. Under the additional constraint of implantation for a prescribed time, this means that decreases in current density with corresponding increases in ion energy result in reductions in the dose delivered onto the material surface. Peak N concentrations tend to be relatively independent of dose (Fig. 2) and this in turn implies that decreases in current density correspond to thinner treated layers. Hence, it is suggested that the optimum implantation energy under the above conditions (~ 1 keV) is the value that produces the maximum thickness. This thickness develops as a consequence of the competing rates of nitrogen supply into the near-surface layer and nitrogen inward diffusion and surface removal via sputtering. The commercial implications of a low implantation energy are significant because capital investment costs and safety concerns are both mitigated by reductions in the operating voltage to the 1-keV level.

These results generally show that layers produced during short (10 and 30 min) implantation times at low implantation energies have excellent load-bearing capabilities (Fig. 5) and reasonable layer thicknesses (Table 1). Further improvements in load-bearing capacity (critical load) are expected for thicker layers (e.g., the 125-min-processing-time case), but they could not be demonstrated because critical loads exceeded the test limit of the machine. Analysis of a large body of data has suggested that layer thickness scales with the square root of the processing time (Williamson et al., 1994) although the 10-min implanted data in this study do not seem to fit that model. These short processing times are, however, noteworthy because they yielded dramatic improvements in critical load while suggesting operating cost reductions relevant to commercial applications.

The data indicate that the preferred implantation temperature is determined by the diffusion and phase-separation kinetics of the material being treated. In the present case, implantation at 400°C for times of order 10 min facilitates rapid N diffusion and solid-solution strengthening of the surface. Further discussion of the formation of this metastable phase including diffusion kinetics are presented in more detail by Williamson et al. (1994). For different types of steels other considerations such as temper softening or rapid diffusion

(e.g., in the bcc phase) may become important considerations in selecting the implantation temperature.

Parameters varied in this study have pertained to nitrogen-ion implantation rather than plasma nitriding because implantation equipment was more readily available and because it afforded precise parameter control. In the case where implantation and nitriding comparisons were made, implantation yielded thicker layers. In another case, not discussed in the text, where hydrogen-ion bombardment did not precede nitriding, the thickness of the N-rich layer was negligible. This result suggests that a surface contaminant (e.g., an oxide) may inhibit the diffusion of low-energy N ions when the disks were nitrided. This contaminant may be removed more effectively by sputtering in the implantation apparatus. It is also possible that continuous sputtering of a N-rich surface layer during processing is important, but probably only in the case where the upper limit on the rate of nitrogen diffusion is more than the rate of N supply.

Conclusions

Nitrogen implantation or plasma nitriding at 400°C induces the formation of nitrogen in solid solution in fcc 304 SS. The thicknesses of the resulting N-rich layers extend far beyond the ballistic implantation range as a result of enhanced thermal-diffusion sustained by a high nitrogen current density. Under the conditions of approximately constant beam-power (a few watts/cm^2), temperature (400°C) and time (10–30 min) at which the tests were performed, the layer thickness was maximized when the incident ion energy was near 1 keV and the implantation current density was near 2.5 mA/cm^2. These surface layers have high hardnesses (near $H_v = 2000$ kgf/mm^2) and are very resistant to sliding wear (wear rate $\leq 10^{-7}$ mm^3/N/m) under high Hertzian-stress conditions. The critical normal load at which the surfaces undergo the mild-to-severe wear transition increases with layer thickness. The reductions in layer thickness and critical load observed when ion energies are reduced below ≈ 1 keV and current densities are increased may be related to surface contamination coupled with low ion-penetration depths at these energies. Differences between plasma nitriding and N-ion implantation may be related to differences in sputtering of surface contaminants for the two processes. An increase in implantation temperature to 475°C enhances diffusion and, therefore, layer growth rate but it also results in phase separation of the 304 SS and the formation of CrN precipitates. Consequently, these layers can be expected to be more susceptible to corrosion.

Acknowledgment

This work was supported by the National Science Foundation and the Department of Energy (Argonne National Laboratory) under grants MSS-9104480, MSS-9116935, and Contract 0372401.

References

Bolster, R. N., and Singer, I. L., 1980, "Surface Hardness and Abrasive Wear Resistance of Nitrogen-Implanted Steels," *Appl. Phys. Lett.*, Vol. 36, pp. 208–209.

Byeli, A. V., Shikh, S. K., and Khatko, V. V., 1992, "Friction and Wear of High Speed Steel Doped with Low Energy Nitrogen Ions," *Wear*, Vol. 159, pp. 185–190.

Chabica, M. E., Williamson, D. L., Wei, R., and Wilbur, P. J., 1992, "Microstructure and Corrosion of Nitrogen-Implanted AISI 304 Stainless Steel," *Surf. and Coat. Technol.*, Vol. 51, pp. 24–29.

Conrad, J. R., Radtke, J. L., Dodd, R. A., Worzala, F. J., and Tran, N. C., 1987, "Plasma Source Ion-Implantation Technique for Surface Modification," *J. Appl. Phys.*, Vol. 62, pp. 4591–4596.

Edenhofer, B., 1974, "Physical Metallurgical Aspects of Ionitriding," *Heat Treatment of Metals*, Vol. 1, pp. 23–28.

Hudis, H., 1973, "Study of Ion-Nitriding," *J. Appl. Phys.*, Vol. 44, pp. 1489–1496.

Hutchings, R., Collins, G. A., and Tendys, J., 1992, "Plasma Immersion Ion Implantation: Duplex Layers from a Single Process," *Surf. and Coat. Technol.*, Vol. 51, pp. 489–494.

Inal, O. T., and Robino, C. V., 1982, "Structural Characterization of Some Ion-Nitrided Steels," *Thin Solid Films*, Vol. 95, pp. 195–207.

Jones, C. K., and Martin, S. W., 1964, "Nitriding, Sintering and Brazing by Glow Discharge," *Met. Prog.*, Vol. 85, pp. 94–98.

Komvopoulos, K., 1989, "Elastic-Plastic Finite Element Analysis of Indented Layered Media," ASME JOURNAL OF TRIBOLOGY, Vol. 111, pp. 430–439.

Peterson, M. B., and Ramalingam, S., 1981, "Coatings for Tribological Applications," in *Fundamentals of Friction and Wear of Materials*, Rigney, D. A., ed., Amer. Soc. of Metals, Metals Park, OH, pp. 331–372.

Rehn, L. E., Averback, R. S., and Okamoto, P. R., 1985, "Fundamental Aspects of Ion Beam Surface Modification: Defect Production and Migration Processes," *Mater. Sci. Eng.*, Vol. 69, pp. 1–11.

Shamim, M., Scheuer, J. T., and Conrad, J. R., 1991, "Measurements of Spatial and Temporal Sheath Evolution for Spherical and Cylindrical Geometries in Plasma Source Ion Implantation," *J. Appl. Phys.*, Vol. 69, pp. 2904–2908.

Singer, I. L., Vardiman, R. G., and Bolster, R. N., 1988, "Polishing Wear Resistance of Ion-Implanted 304 Steel," *J. Mater. Res.*, Vol. 3, pp. 1134–1143.

Strack, H., 1963, "Ion Bombardment of Silicon in a Glow Discharge," *J. Appl. Phys.*, Vol. 34, pp. 2405–2409.

Szasz, A., Fabian, D. J., Hendry, A., and Szaszne-Csih, Z., 1989, "Nitriding of Stainless Steel in an r-f Plasma," *J. Appl. Phys.*, Vol. 66, pp. 5598–5601.

Tendys, J., Donnelly, I. J., Kenny, M. J., and Pollock, J. T. A., 1988, "Plasma Immersion Ion Implantation Using Plasmas Generated by Radio Frequency Techniques," *Appl. Phys. Lett.*, Vol. 53, pp. 2143–2145.

Wei, R., Wilbur, P. J., Sampath, W. S., Williamson, D. L., Qu, Y., and Wang, L., 1990, "Tribological Studies of Ion-Implanted Steel Constituents using as Oscillating Pin-on-Disc Wear Tester," ASME JOURNAL OF TRIBOLOGY, Vol. 112, pp. 27–36.

Wei, R., Wilbur, P. J., Ozturk, O., and Williamson, D. L., 1991a, "Tribological Studies of Ultrahigh-Dose, Nitrogen Implanted Iron and Stainless Steel," *Nucl. Instrum. Meth. Phys. Res.*, Vol. B59/60, pp. 731–736.

Wei, R., Wilbur, P. J., Sampath, W. S., Williamson, D. L., and Wang, L., 1991b, "Effects of Ion Implantation Conditions on the Tribology of Ferrous Surfaces," *Lubr. Eng.*, Vol. 47, pp. 326–334.

Wilbur, P. J., and Daniels, L. O., 1985, "The Development and Application of an Ion Implanter Based on Ion Thruster Technology," *Vacuum*, pp. 5–9.

Williamson, D. L., Wang, L., Wei, R., and Wilbur, P. J., 1990, "Solid Solution Strengthening of Stainless Steel Surface Layers by Rapid, High-Dose, Elevated Temperature Nitrogen Ion Implantation," *Mat. Lett.*, Vol. 9, pp. 302–308.

Williamson, D. L., Ozturk, O., Glick, S., Wei, R., and Wilbur, P. J., 1991, "Microstructure of Ultrahigh-Dose, Nitrogen Implanted Iron and Stainless Steel," *Nucl. Instrum. Meth. in Phys. Res.*, Vol. B59/60, pp. 737–741.

Williamson, D. L., Ivanov, I., Wei, R., and Wilbur, P. J., 1992, "Role of Chromium in High-Dose, High-Rate, Elevated Temperature Nitrogen Implantation of Austenitic Stainless Steels," *Mat. Res. Soc. Symp. Proc.*, Vol. 235, pp. 473–478.

Williamson, D. L., Ozturk, O., Wei, R., and Wilbur, P., 1994, "Metastable Phase Formation and Enhanced Diffusion in f.c.c. Alloys under High Dose, High Flux Nitrogen Implantation at High and Low Ion Energies," *Surf. and Coat. Technol*, Vol. 65, pp. 15–23.

Yost, F. G., Picraux, S. T., Follstaedt, D. M., Pope, L. E., and Knapp, J. A., 1983, "The Effects of N^+ Implantation on the Wear and Friction of Type 304 and 15-5PH Stainless Steel," *Thin Solid Films*, Vol. 107, pp. 287–295.

Zhang, Z. L., and Bell, T., 1985, "Structure and Corrosion Resistance of Plasma Nitrided Stainless Steel," *Surf. Eng.*, pp. 131–135.

Ziegler, J. F., Biersack, I. P., and Littmark, U., 1985, "Stopping and Range of Ion In Solids," *The Stopping and Range of Ions in Matter*, Vol. 1, Ziegler, J. F., ed., Pergamon Press, New York.